

Coordination of cell proliferation and anterior-posterior axis establishment in the mouse embryo

Daniel W. Stuckey^{1,*}, Melanie Clements^{1,*}, Aida Di-Gregorio¹, Claire E. Senner^{1,‡}, Paul Le Tissier², Shankar Srinivas^{3,†} and Tristan A. Rodriguez^{1,†}

SUMMARY

During development, the growth of the embryo must be coupled to its patterning to ensure correct and timely morphogenesis. In the mouse embryo, migration of the anterior visceral endoderm (AVE) to the prospective anterior establishes the anterior-posterior (A-P) axis. By analysing the distribution of cells in S phase, M phase and G2 from the time just prior to the migration of the AVE until 18 hours after its movement, we show that there is no evidence for differential proliferation along the A-P axis of the mouse embryo. Rather, we have identified that as AVE movements are being initiated, the epiblast proliferates at a much higher rate than the visceral endoderm. We show that these high levels of proliferation in the epiblast are dependent on Nodal signalling and are required for A-P establishment, as blocking cell division in the epiblast inhibits AVE migration. Interestingly, inhibition of migration by blocking proliferation can be rescued by Dkk1. This suggests that the high levels of epiblast proliferation function to move the prospective AVE away from signals that are inhibitory to its migration. The finding that initiation of AVE movements requires a certain level of proliferation in the epiblast provides a mechanism whereby A-P axis development is coordinated with embryonic growth.

KEY WORDS: Anterior-posterior axis establishment, Nodal signalling, Mouse embryo, Proliferation, Anterior visceral endoderm

INTRODUCTION

The anterior visceral endoderm (AVE) is an extra-embryonic signalling centre that establishes the anterior-posterior (A-P) axis of the mouse embryo. The AVE forms at the distal tip of the embryo at 5.25 days post-coitum (dpc) by a combination of inductive signalling by the Tgfb factors Nodal (Brennan et al., 2001) and activin (Yamamoto et al., 2009) and inhibitory signalling by the extra-embryonic ectoderm (Rodriguez et al., 2005; Yamamoto et al., 2009). At 5.5 dpc, cells from the AVE undergo a unidirectional movement from the distal tip of the embryo to the future anterior side. This movement is essential for correct positioning of the A-P axis (Srinivas, 2006; Takaoka et al., 2007).

Although the precise mechanism of how cells of the AVE move from the distal tip [where they are termed distal visceral endoderm (DVE)] to the prospective anterior is not well understood, two alternative hypotheses have been proposed. Time-lapse imaging studies have suggested that AVE movements are part of an active migration process (Srinivas et al., 2004). The findings that *Nap1* (Nckap1 – Mouse Genome Informatics; a component of the WAVE complex that is essential for cell migration) and the small GTPase *Rac1* are required for AVE movements (Migeotte et al., 2010; Rakeman and Anderson, 2006) and that canonical Wnt signalling

and its antagonists act as guidance cues for AVE migration (Kimura-Yoshida et al., 2005) have supported this hypothesis. In contrast to these findings, BrdU-incorporation studies coupled with embryo transfection experiments have led to the proposal that differential proliferation within the VE, modulated by Nodal signalling, provides the driving force for AVE movements. According to this model, Nodal signalling is required for proliferation within the VE, and prospective AVE cells are displaced because of the differential rate of proliferation that is created when Nodal activity is antagonised only in the anterior of the embryo by *Lefty1* and *Cerberus-like* (*Cer1* or *Cer11*) (Yamamoto et al., 2004). However, further experiments are required to clarify the relative contributions of both these processes to the movements of the AVE.

Concurrent with AVE movements, the underlying epiblast undergoes rapid proliferation. It has been calculated that there is a 4.5- to 5-fold increase in epiblast cell number between 5.5 and 6.5 dpc, with the epiblast requiring ~660 cells for gastrulation to commence (Snow, 1977). Formation of the primitive streak at the prospective posterior of the embryo at 6.5 dpc marks the initiation of gastrulation and this dramatic rise in epiblast cell number is required to sustain the recruitment of ectoderm cells through the primitive streak. This suggests coordination between epiblast growth and posterior patterning of the embryo.

What factors are responsible for maintaining proliferation in the early embryo? *Nodal* mutant embryos are smaller than controls (Camus et al., 2006; Mesnard et al., 2006) and it has been reported that Nodal promotes cell proliferation in the VE (Yamamoto et al., 2004). *Bmpr1a* mutant embryos show epiblast proliferation defects (Mishina et al., 1995), implicating BMP signalling in the maintenance of proliferation in the early post-implantation embryo. Indeed, BMP signalling is required to sustain Nodal signalling in the epiblast (Ben-Haim et al., 2006; Di-Gregorio et al., 2007), suggesting that these two signalling pathways might cooperate to sustain epiblast proliferation.

¹Molecular Embryology Group, MRC Clinical Sciences Centre, Imperial College London, Hammersmith Hospital Campus, Du Cane Road, London W12 0NN, UK.

²National Institute for Medical Research, Mill Hill, London NW7 1AA, UK. ³University of Oxford, Department of Physiology Anatomy and Genetics, Le Gros Clark Building, South Parks Road, Oxford OX1 3QX, UK.

*These authors contributed equally to this work

[‡]Present address: Department of Biochemistry, University of Oxford, South Parks Road, Oxford OX1 3QU, UK

[†]Authors for correspondence (shankar.srinivas@dpag.ox.ac.uk; tristan.rodriguez@csc.mrc.ac.uk)

To address the impact of proliferation on A-P axis establishment, we have carried out a detailed analysis of the proliferation patterns within the VE and epiblast at the time of AVE movements. We have studied how this proliferation is regulated and tested its importance for the establishment of the A-P axis in the mouse embryo.

MATERIALS AND METHODS

Mouse strains and embryo recovery

Mice carrying the *Hex*-GFP transgene (Rodriguez et al., 2001) and the CAG-geminin-GFP reporter transgene (Sakaue-Sawano et al., 2008) have been described previously. Embryos were dissected in M2 as described (Nagy et al., 2003). Mice were maintained and treated in accordance with the Home Office's Animals (Scientific Procedures) Act 1986.

Immunohistochemistry and whole-mount in situ hybridisation (WISH)

Hex-GFP embryos were sorted for the presence of GFP and fixed in 4% paraformaldehyde overnight at 4°C. Standard protocols for immunohistochemistry (Nagy et al., 2003) were used for rabbit anti-phospho-histone H3 (Ser28) (Upstate, 07-145; diluted 1:500), PcnA (Abcam; 1:500) and Ki67 (Abcam; 1:500) and for WISH (Thomas and Beddington, 1996). A sodium citrate antigen-retrieval step was carried out for Ki67 and PcnA. Stained embryos were placed in glass-bottom microwell dishes (MatTek, USA) in a drop of 1:1 glycerol:PBS. Confocal images of the embryo were captured on a Leica DM IRB inverted confocal microscope through either a 10×/0.30 PH1 air objective or a 40×/1.00 PH3 oil-immersion objective. z-stacks were taken at 4-µm intervals through the embryo, with each channel acquired sequentially. Stacks were then merged and reconstructed using ImageJ 1.33u.

Whole-mount GFP and BrdU staining

A modification of the protocol available on the Rossant Laboratory web page (www.sickkids.ca/research/rossant/protocols/BrdU_embryoStain.asp) was used. Briefly, *Hex*-GFP embryos were cultured in 20 µM BrdU in 80 µl drops of 1:1 DMEM:fetal calf serum covered by mineral oil at 37°C, 5% CO₂ for 15 or 30 minutes, washed 3× 5 minutes in PBS and fixed in 4% paraformaldehyde containing 2 mM EGTA for 1.5 hours at 4°C. Embryos were then washed in PBT (PBS containing 0.1% Tween 20) for 1 hour at 4°C and blocked in PBS containing 10% normal goat serum and 0.1% Triton X-100 at room temperature (RT) for 1.5 hours. Embryos were then incubated with rabbit anti-GFP antibody (Molecular Probes, A11122) diluted 1:1000 in blocking solution at 4°C for a minimum of 2 days. Embryos were washed 3× 5 minutes plus 1× 1 hour at RT in 0.1% Triton X-100 and incubated in Alexa Fluor 488 goat anti-rabbit IgG (Molecular Probes, A11008) diluted to 1:500 with blocking solution for 2 hours at RT with rocking. Embryos were washed 3× 5 minutes plus 1× 1 hour at RT, post-fixed in 4% paraformaldehyde for 10 minutes and transferred to 2 M HCl in PBS containing 0.1% Tween 20 for 30 minutes at 37°C to denature the DNA. The HCl was quenched by washing 3× 5 minutes in borate buffer (0.1 mM, pH 8.5) at RT, blocked in MABT (100 mM maleic acid pH 7.5, 150 mM NaCl, 0.1% Tween 20) containing 10% sheep serum for a minimum of 1.5 hours at RT. The embryos were then incubated overnight in rat anti-BrdU (Abcam, ab6326) diluted 1:100 in MABT containing 1% sheep serum at RT with constant rocking. The following day, embryos were washed 3× 5 minutes in MABT containing 10% sheep serum and 5× 1 hour in MABT at RT. Embryos were incubated in polyclonal Cy3 goat anti-rat IgG (Abcam, ab6953) diluted 1:500 with the same blocking solution and incubated at 4°C overnight. Finally, embryos were washed 5× 1 hour in MABT and stained with To-pro-3 iodide (Molecular Probes, T3605) diluted 1:500, mounted and images acquired.

Inhibitor cultures and growth factor treatment

Hex-GFP embryos were cultured in 200 nM nocodazole (Sigma) (MacAuley et al., 1993; Vasquez et al., 1997), 200 nM nocodazole plus 500 µg/ml Dkk1 (R&D Systems), 150 µM genistein (DiPaola, 2002), 2.5 µM hydroxyurea (Engstrom et al., 1979) (Sigma) or 10 µM SB-431542 (Inman et al., 2002) in pre-equilibrated drops. Each 80 µl drop comprised inhibitor

diluted in 1:1 DMEM:rat serum covered with mineral oil. Embryos were incubated at 37°C, 5% CO₂ overnight (typically 16 hours) or for 2 hours (see Fig. S4 in the supplementary material), then washed 3× 5 minutes in PBS and fixed in 4% paraformaldehyde overnight at 4°C. Embryos then underwent staining as described above. In the case of BrdU treatment of embryos cultured in SB-431542, 20 µM BrdU was added for the last 30 minutes of culture and then embryos were stained as described above.

Statistical analysis

Cells were scored using the ImageJ cell counter. The non-parametrical χ^2 test was used in Fig. 2 to test the difference between the sample (number of dividing cells in each quadrant) and expected distribution if proliferation were similar in all regions of the embryo (each quadrant is assumed to represent 25% of dividing cells). *t*-tests were applied to the data in the remaining figures. This parametric test is based on the assumption that the samples come from populations that are normally distributed using continuous, not discrete, numerical data. The unpaired *t*-test assumes that the two data sets being compared are independent and identically distributed (i.e. from different embryos but both normally distributed).

RESULTS

Not all AVE cells move together to the anterior of the embryo

As a starting point to study whether differential proliferation could be the driving force for AVE movements, time-lapse imaging of *Hex*-GFP embryos (which have a fluorescently labelled AVE) was carried out (Rodriguez et al., 2001). The positions of GFP-positive cells at the leading (anterior) and lagging (posterior) fronts of the *Hex*-GFP domain were analysed at the onset of AVE movements. As the anterior AVE cells moved proximally, some GFP-positive cells remained distal (Fig. 1A) and did not migrate in the time frame that it took the leading cells to reach the embryonic/extra-embryonic boundary. This result suggests that at least the leading AVE cells are not passively displaced to the anterior of the embryo by increased proliferation in the GFP-negative posterior part of the VE.

Random distribution of S-phase cells within the VE at the time of AVE movements

We set out to examine in greater detail the proliferation rates of different regions of the VE during the time that AVE movements are occurring. As a first step, we determined the overall levels of proliferation in the anterior and posterior VE by analysing the distribution of Ki67-positive cells, a protein that is expressed in all proliferating cells (Chenn and Walsh, 2002). At 5.75 dpc, 97.5±1.18% of *Hex*-GFP AVE cells were Ki67 positive, compared with 94.2±2.59% of posterior VE cells. At 6.25 dpc, 99.46±0.61% of AVE cells were labelled, as compared with 98.72±0.81% of posterior VE cells (see Fig. S1 in the supplementary material). This indicates that very few cells in any region of the VE are not in the cell cycle.

To analyse the distribution of cells in S phase we studied the pattern of BrdU incorporation in the VE of 5.5-dpc embryos. *Hex*-GFP embryos were given a 15-minute BrdU pulse and then divided into three groups according to GFP expression: the pre-distal group displayed a low level of GFP expression throughout the VE (Fig. 1B); the distal group included those embryos in which the DVE had resolved to the distal tip (Fig. 1D); and the tilted group showed a clear asymmetric tilt of the DVE (Fig. 1F). The numbers of BrdU-positive nuclei were counted and expressed as a percentage of the total cell number, referred to as the incorporation index. In the pre-distal group, the mean incorporation index of the VE was 76±2.66% (Fig. 1C), with non-BrdU-incorporating nuclei not

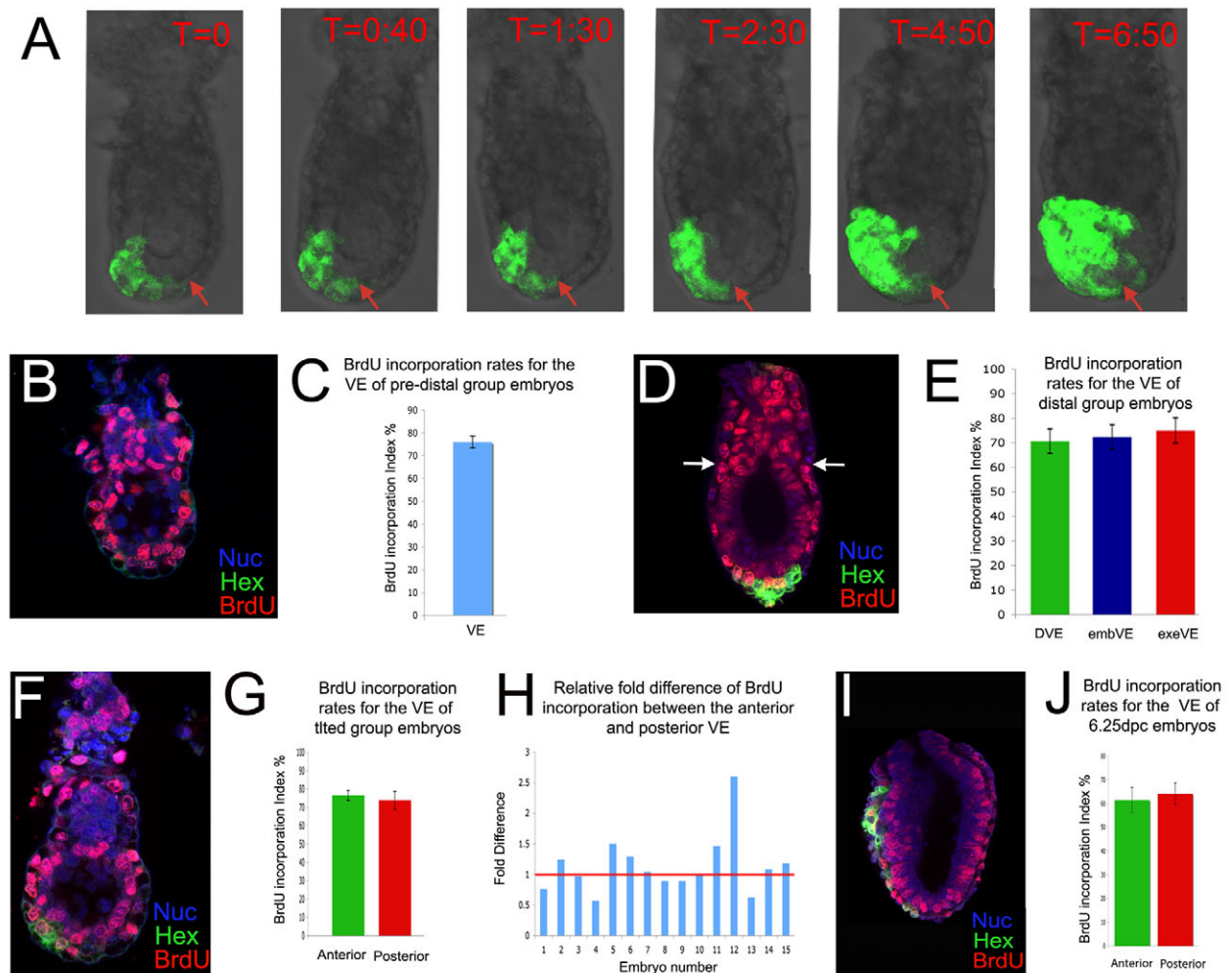


Fig. 1. Random distribution of S-phase cells in the VE at the time of AVE migration. (A) Stills taken from a time-lapse movie of a *Hex*-GFP mouse embryo showing how GFP-positive cells remain at the distal tip of the embryo (red arrow) when leading cells of the anterior visceral endoderm (AVE) domain are migrating. Time is shown in hours:minutes. (B) BrdU staining of a pre-distal *Hex*-GFP embryo. Nuc, TOPO-3 staining of DNA. (C) BrdU incorporation index in pre-distal group embryos. Results are mean \pm s.e.m.; $n=5$. (D) BrdU staining of a distal *Hex*-GFP embryo. Arrows indicate the embryonic/extra-embryonic boundary. (E) BrdU-incorporation index in distal group embryos for the distal visceral endoderm (DVE), embryonic VE (embVE) and extra-embryonic VE (exeVE) domains (see Fig. 2B). Results are mean \pm s.e.m.; $n=6$. (F) BrdU staining of a tilted group *Hex*-GFP embryo. (G) BrdU-incorporation index of the anterior and posterior VE of tilted group embryos. Results are mean \pm s.e.m.; $n=11$. (H) Relative fold difference in BrdU incorporation between the anterior and posterior VE regions of tilted group embryos. The red line indicates no relative difference between the two areas. The relative fold difference values 1-15 are 0.76, 1.24, 0.97, 0.57, 1.50, 1.29, 1.04, 0.89, 0.89, 0.98, 1.46, 2.60, 0.62, 1.08 and 1.18. (I) BrdU staining of a 6.25-dpc *Hex*-GFP embryo. (J) BrdU-incorporation index in the anterior and posterior VE of 6.25-dpc embryos. Results are mean \pm s.e.m.; $n=11$. There were no significant differences between the anterior and posterior VE by Student's *t*-test for paired samples ($P>0.05$).

appearing to cluster in any particular region of the VE. Regional division of the embryonic VE was not possible at this stage because GFP expression was throughout the VE (Fig. 1B).

Although an A-P axis could not be assigned to the distal group, embryos were divided into DVE, embryonic VE (embVE) and extra-embryonic VE (exeVE) domains (Fig. 1D). The mean incorporation index of these areas was quantified and found to be very similar: DVE, $68.38 \pm 4.81\%$; embVE, $70.07 \pm 4.91\%$; and exeVE, $72.63 \pm 4.97\%$ (Fig. 1E).

The tilted group could be assigned an A-P axis and the embVE was divided into anterior and posterior halves according to position relative to the DVE (*Hex*-GFP domain). There was no significant difference in the mean incorporation index of the anterior (76.54 ± 2.68) and posterior ($73.84 \pm 4.74\%$) VE (Fig. 1G). To ascertain if there were any regional differences within the anterior

VE, this region was further subdivided into VE anterior to the DVE and DVE. Again, both these areas showed very similar incorporation indexes: VE anterior to the DVE, $80.78 \pm 3.18\%$; DVE, $74.44 \pm 3.63\%$ (see Fig. S2A,B in the supplementary material). Next, the ratio of the anterior to posterior VE proliferation index was plotted for each embryo to analyse the variability that might exist between embryos. A value exceeding 1 indicated more proliferation in the anterior than posterior VE, whereas a value of less than 1 indicated the converse. Of the 15 embryos in the group, eight displayed values exceeding 1 and seven had values below 1 (Fig. 1H), which is inconsistent with there being increased proliferation in the posterior as compared with the anterior VE. Therefore, when the DVE movements are being initiated, the distribution of cells in S phase is not significantly different between the anterior and posterior VE.

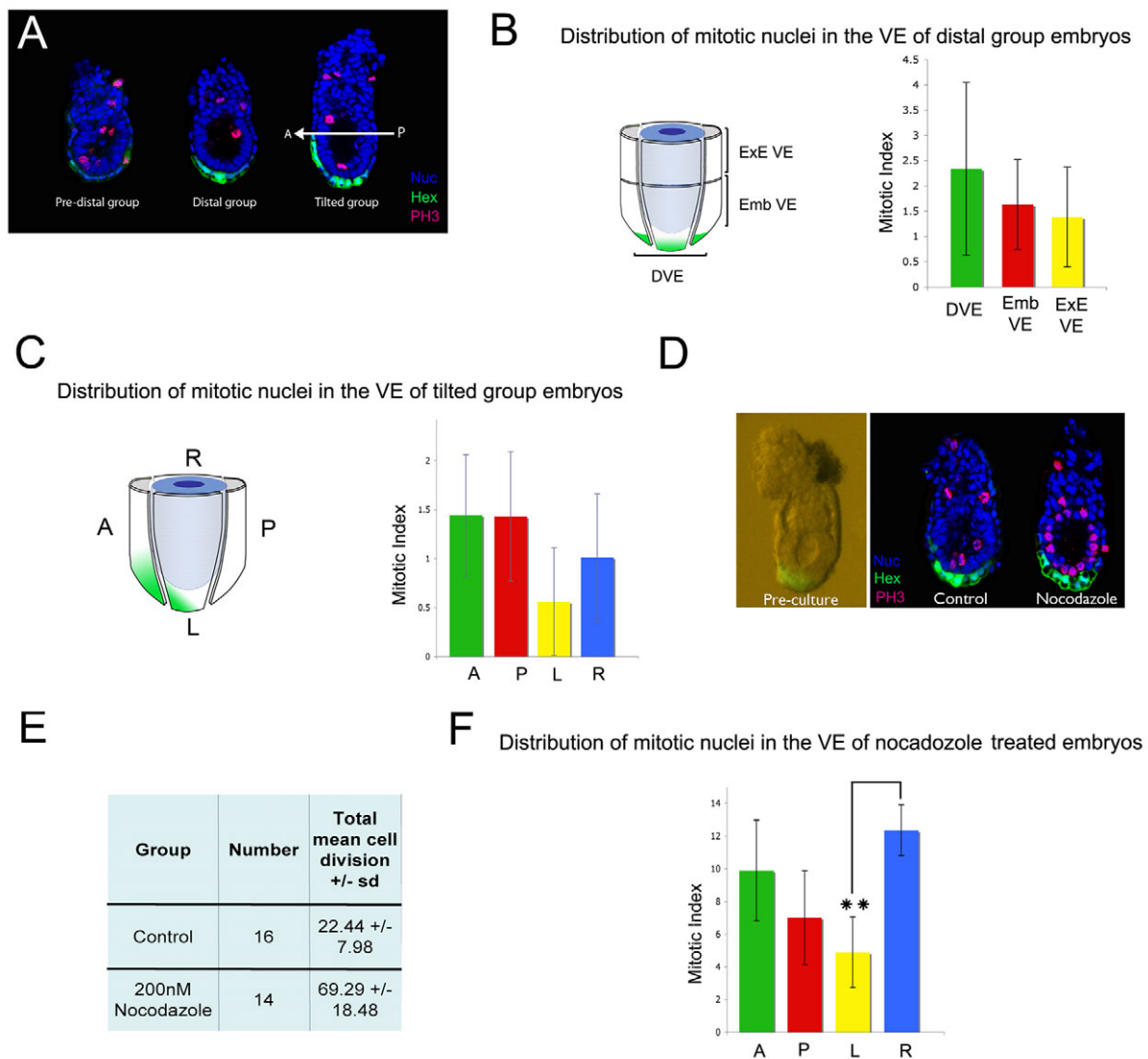


Fig. 2. Random distribution of mitotic cells at the onset of AVE migration. (A) Phospho-histone-H3 (PH3) staining of pre-distal, distal and tilted group *Hex*-GFP mouse embryos. The A-P axis is indicated. (B) The VE of six distal embryos was divided into three regions (DVE, embVE and exeVE) as illustrated. The mean mitotic index was calculated for each of these regions. Results are mean \pm s.e.m.; $n=6$. (C) The VE of five tilted group embryos was divided into anterior (A), posterior (P), lateral left (L) and lateral right (R) quadrants. The mean mitotic index was calculated for each of these regions. Results are mean \pm s.e.m.; $n=5$. (D) 5.5-dpc *Hex*-GFP embryos were cultured in the presence of nocodazole (200 nM) to cause mitotic arrest. Embryos were stained for PH3 and nuclei visualised with DAPI. (E) Treatment with nocodazole caused a 3-fold accumulation of mitotic cells (control, $n=16$; treated, $n=14$). (F) The VE of these embryos was divided into A, P, L and R quadrants and the mean mitotic index of each quadrant calculated. There was a statistically significant difference between the L and R quadrants (** $P<0.01$, χ^2 test).

Random distribution of M-phase cells along the A-P axis at the time of AVE movements

To confirm that our BrdU data accurately reflect the distribution of proliferating cells, we analysed the distribution of cells in M phase within the VE between 5.25 and 5.75 dpc using an anti-phospho-histone-H3 (PH3) antibody. Embryos were grouped as before according to the position of the *Hex*-GFP domain (Fig. 2A), and the mitotic index (percentage of mitotic cells; see Table S1 in the supplementary material) was calculated for the different regions of the VE. In the distal group there was no significant difference in the mitotic index of the DVE ($2.34 \pm 1.71\%$), embVE ($1.33 \pm 0.99\%$) and exeVE ($1.63 \pm 0.89\%$; Fig. 2B). In the tilted group the mean mitotic index was similar in the anterior and posterior quadrants ($1.44 \pm 0.62\%$ and

$1.43 \pm 0.66\%$), which were higher, although not significantly so, than those of the lateral quadrants (right, $1.01 \pm 0.65\%$; left, $0.56 \pm 0.55\%$).

To rule out the possibility that a proliferative burst within the VE might have been missed in the previous experiment, embryos were cultured for 4 hours in the presence of the mitotic inhibitor nocodazole (MacAuley et al., 1993; Vasquez et al., 1997) just as DVE movements are being initiated. This caused a 3-fold accumulation in the proportion of mitotic cells (Fig. 2D,E). When the mitotic index was calculated for each quadrant in these nocodazole-treated embryos (Fig. 2F), there was no significant difference between the anterior ($9.89 \pm 3.08\%$) and posterior ($7.01 \pm 2.86\%$) quadrants. To test whether there were any regional differences within the anterior VE, this region was further

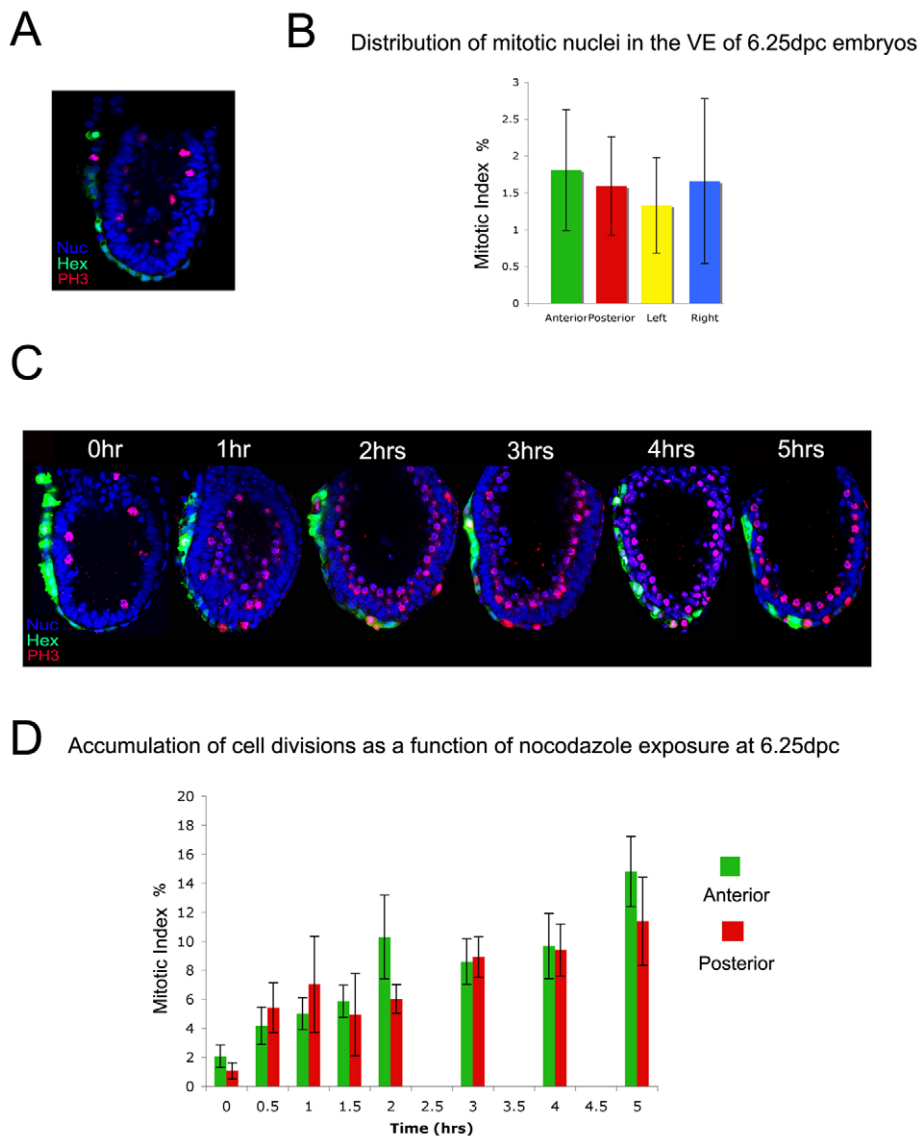


Fig. 3. Cell cycle rates in the AVE and posterior VE. (A) PH3 staining of 6.25-dpc *Hex*-GFP mouse embryos. (B) The embVE of six 6.25-dpc embryos was divided into A, P, L and R quadrants (see Fig. 2C). The mean mitotic index for each of these regions was calculated. Results are mean \pm s.e.m.; $n=6$. No significant differences were observed between quadrants as assessed by χ^2 test. (C) 6.25-dpc embryos were treated with nocodazole for up to 5 hours and stained for PH3 to analyse the accumulation of mitotic nuclei. (D) Accumulated mitotic nuclei in the AVE and posterior VE were quantified in each embryo and the mean mitotic indexes were plotted as a function of length of nocodazole exposure. Results are mean \pm s.e.m.; 0 hours, $n=11$; 0.5 hours, $n=6$; 1 hour, $n=11$; 1.5 hours, $n=8$; 2 hours, $n=9$; 3 hours, $n=10$; 4 hours, $n=6$; 5 hours, $n=4$. No significant differences in mitotic index between anterior and posterior VE were observed as assessed by χ^2 test (B) and a Student's *t*-test for paired samples ($P>0.05$; D).

subdivided into VE anterior to the DVE and DVE, as described above. We again found that the mitotic index of these anterior regions was not significantly lower than that of the posterior VE: VE anterior to the DVE, $11.82\pm 5.45\%$; DVE, $6.15\pm 1.66\%$ (see Fig. S2C,D in the supplementary material). By contrast, when we compared the lateral quadrants we found that the mean mitotic index of the lateral right quadrant was significantly higher ($12.36\pm 1.54\%$) than that of the lateral left quadrant ($4.89\pm 2.16\%$; $P<0.01$), suggesting that proliferation on the right side of the embryo is greater than on the left. In conclusion, we observe little difference between the proliferation rates of the anterior and posterior VE and it is therefore unlikely that the first cells of the AVE initiate their movements by being displaced as a result of differential proliferation rates.

The anterior and posterior VE have similar proliferation rates at 6.25 dpc

It is possible that differential proliferation within the VE could be responsible for the movement of AVE cells that do not migrate with the leading edge of the AVE at 5.5 dpc. To test this hypothesis, 6.25-dpc embryos were labelled with BrdU for 30

minutes and the incorporation index was calculated (Fig. 11,J). The AVE (all anterior VE cells) had a mean incorporation index of $61.44\pm 5.25\%$, a similar value to the $64.13\pm 4.61\%$ obtained for the rest of the VE (Fig. 1J), suggesting no A-P difference in proliferation.

To further assess the regional distribution of mitotic cells within the embryonic VE at 6.25 dpc, PH3-stained embryos were analysed (Fig. 3A,B). The anterior quadrant had a mitotic index of $1.81\pm 0.82\%$, the posterior quadrant $1.59\pm 0.67\%$, the lateral left quadrant $1.33\pm 0.65\%$ and the lateral right quadrant $1.66\pm 1.12\%$. This small variation in mitotic index between quadrants was not statistically significant, suggesting that the low levels of cell division within the VE at 6.25 dpc show no regional bias. However, we cannot exclude the possibility that local proliferation differences do exist within the subdomains analysed.

To determine whether there was any difference between the cell cycle rates of the AVE and the rest of the VE, 6.25-dpc *Hex*-GFP embryos were cultured in nocodazole for intervals of 0-5 hours (Fig. 3C). The mitotic index of the VE was calculated for each embryo at each time point and the percentage of cells in mitosis was plotted as a function of time in the presence of nocodazole

(Fig. 3D). There was no significant difference between the division rates of the anterior and posterior VE at any of the time points studied, indicating that cells of the AVE cycle at a similar rate to those in the rest of the VE.

This random distribution of cells in S phase and in M phase contrasts with a previous report of no BrdU incorporation in the AVE at 6.5 dpc (Yamamoto et al., 2004). We therefore confirmed that there were no significant differences between the proliferation rates of cells in the AVE and posterior VE by analysing the distribution of cells positive for PcnA (a marker of cells in G1-S) (Connolly and Bogdanffy, 1993; Takahashi and Caviness, 1993). At 6.25 dpc we observed very similar levels of PcnA-positive cells between the anterior and posterior VE ($89.00 \pm 2.83\%$ and $83.85 \pm 4.70\%$, respectively; see Fig. S3 in the supplementary material). We also analysed the distribution of geminin-positive cells using a transgene carrying a CAG-geminin-GFP reporter. This transgene shows highest GFP expression during the late S phase and G2 phases of the cell cycle (Sakaue-Sawano et al., 2008). We found no significant difference in the numbers of GFP-positive cells between the anterior and posterior VE ($12.77 \pm 2.24\%$ and $14.08 \pm 3.17\%$, respectively; see Fig. S3 in the supplementary material) of 6.25-dpc embryos using this reporter. Together, these results argue against the hypothesis that, at any time point, migration of AVE cells is driven by differential proliferation within the VE.

Regional distribution of dividing cells in the epiblast between 5.25 and 6.25 dpc

To study how proliferation rates change within the epiblast as AVE movements are initiated, we analysed PH3-stained *Hex*-GFP embryos and determined the mitotic index for this tissue in pre-distal, distal and tilted group embryos (Fig. 4A). We found little variation in the mitotic index of the epiblast between these stages (pre-distal group, $8.05 \pm 1.31\%$; distal group, $8.68 \pm 1.43\%$; tilted group, $7.96 \pm 1.23\%$). This contrasts with a significant decrease in mitotic levels within the VE during this period ($3.65 \pm 1.17\%$, $1.56 \pm 0.68\%$, $0.72 \pm 0.29\%$, respectively; $P < 0.02$). These data indicate that whereas the proliferation rate of the epiblast is 2.2-fold that of the VE prior to AVE induction, when AVE movements are initiated it is 11-fold that of the VE, creating a severe growth imbalance between these tissues. By 6.25 dpc, the overall level of proliferation in the epiblast had dropped and the difference in proliferation rates between the epiblast and VE had fallen to a value similar to that prior to AVE migration (3.7-fold; epiblast, $5.74 \pm 0.84\%$; VE, $1.56 \pm 0.66\%$; Fig. 4A).

The regional distribution of mitotic nuclei in the epiblast at 5.5 dpc was examined (Fig. 4B). When the mean mitotic indexes of the anterior and posterior epiblast of tilted group embryos were compared, no significant difference was observed (anterior, $7.13 \pm 1.24\%$; posterior, $8.31 \pm 1.57\%$). The proliferation rates of the proximal ($9.06 \pm 1.50\%$) and distal ($5.36 \pm 1.27\%$) epiblast were also not significantly different (Fig. 4B). Finally, the right quarter of the epiblast had a significantly greater mitotic index ($5.06 \pm 0.57\%$) than the left quarter of the epiblast ($2.41 \pm 0.63\%$; $P < 0.01$; Fig. 4B). This observation, combined with the fact that a similar trend is seen within the VE (Fig. 2F), indicates a higher proliferation rate on the right side of the embryo at 5.5 dpc.

We repeated this analysis at 6.25 dpc (Fig. 4C) and found no significant difference between the mitotic indexes of the anterior ($6.46 \pm 0.75\%$) and posterior ($6.61 \pm 0.55\%$) epiblast or between the left ($2.93 \pm 1.05\%$) and right ($4.02 \pm 0.62\%$) epiblast. However, the proximal epiblast had a significantly higher mitotic index

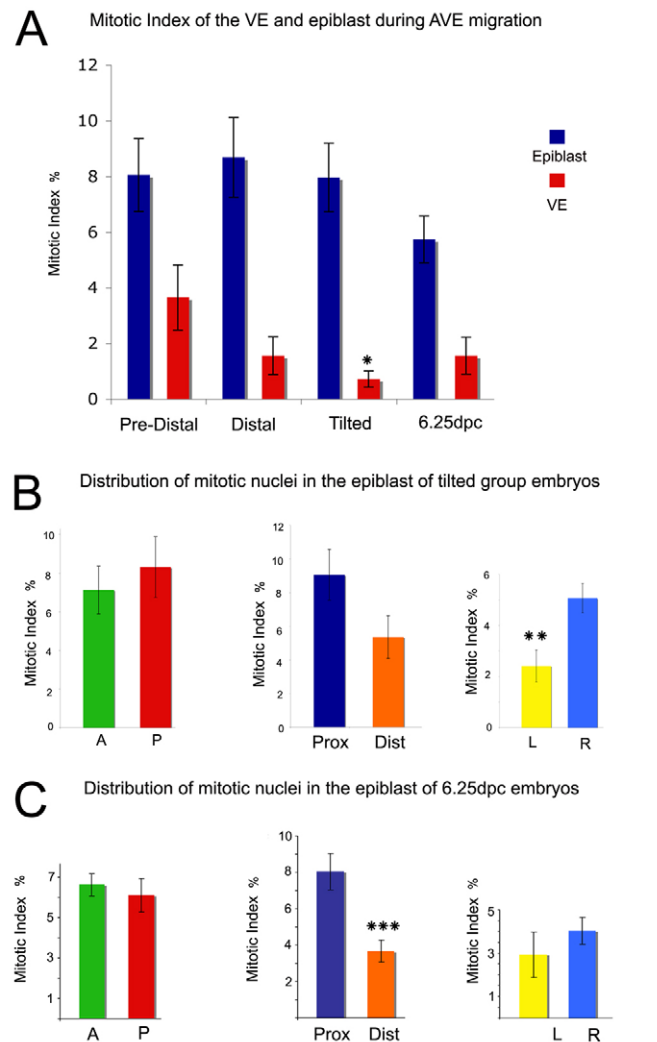
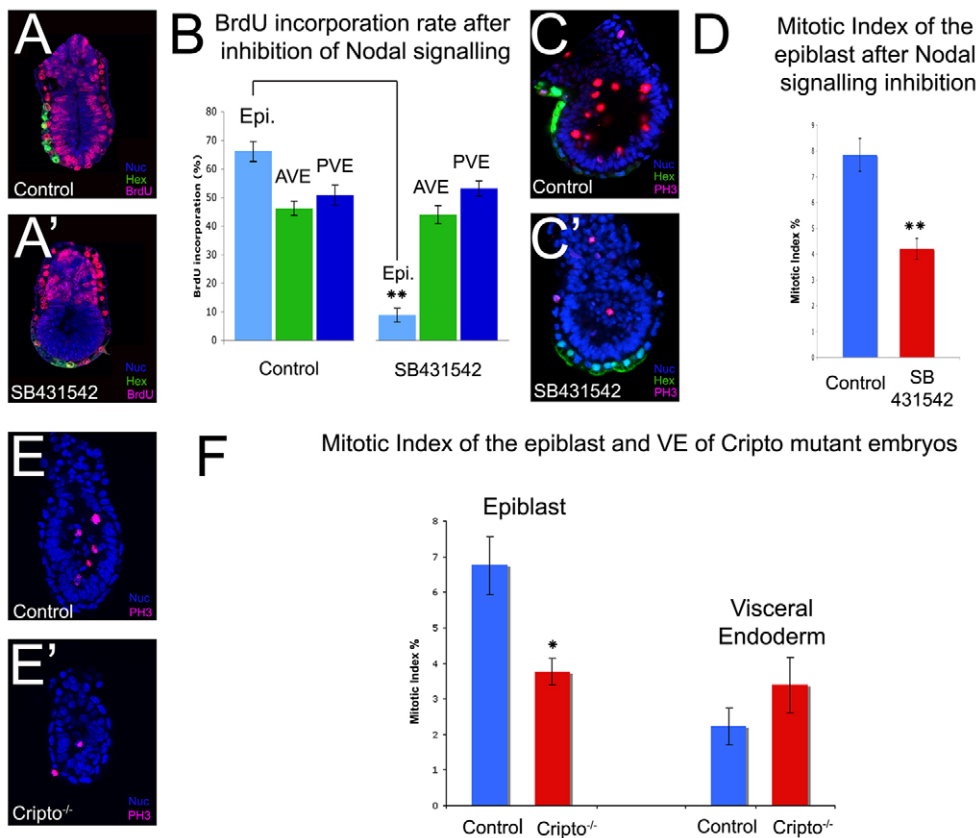


Fig. 4. Distribution of mitotic cells between 5.25 and 6.25 dpc. (A) Differences in the mean mitotic index between the epiblast and VE of PH3-stained pre-distal ($n=5$), distal ($n=5$) and tilted ($n=8$) groups and 6.25-dpc ($n=11$) mouse embryos. (B) The epiblast of five PH3-stained *Hex*-GFP tilted group embryos was divided into anterior (A) and posterior (P) halves, proximal (Prox) and distal (Dist) halves or left (L) and right (R) halves and the mean mitotic index calculated. (C) The epiblast of seven PH3-stained *Hex*-GFP embryos was divided as in B and the mean mitotic index calculated. All results are mean \pm s.e.m. * $P < 0.05$, ** $P < 0.01$, *** $P < 0.001$ by Student's *t*-test for paired samples.

($8.01 \pm 1.01\%$) than the distal epiblast ($3.67 \pm 0.61\%$; $P < 0.005$), which correlates with this being the site of initiation of primitive streak formation, a tissue that will subsequently exhibit a higher rate of proliferation (MacAuley et al., 1993; Snow, 1977).

Nodal signalling is required for AVE migration, maintenance of AVE markers and proliferation in the epiblast

Nodal signalling has been shown to be required for the movements of AVE cells (Norris et al., 2002) by driving differential proliferation within the VE (Yamamoto et al., 2004). Given that we observe no evidence for differential proliferation within the VE at the time of AVE movements, we revisited the requirements for Nodal in these movements. *Hex*-GFP embryos at 5.5 dpc were



cultured overnight in the presence of SB-431542, a small-molecule inhibitor of the Nodal receptor (Inman et al., 2002). This resulted in a complete lack of AVE migration (Fig. 5A'), confirming that Nodal signalling is required for AVE movements. Proliferation was determined in these embryos by BrdU incorporation. Once again, embryos were subdivided into three regions: the GFP-positive AVE, the GFP-negative VE and the epiblast (Fig. 5A-B). In control embryos, the mean BrdU-incorporation index of the AVE (46.23±2.49%) was similar to that of the rest of the VE (50.85±3.47%) and lower than that of the epiblast (66.26±3.25%), reflecting the shorter cell cycle length in the epiblast. Interestingly, after inhibition of Nodal signalling there was little change in the BrdU-incorporation indexes of the AVE (43.97±3.17%) and the rest of the VE (53.12±2.60%), but the incorporation rate of the epiblast had dropped dramatically when compared with controls (8.78±2.43%; $P < 0.0001$). This indicates that whereas proliferation in the epiblast is Nodal dependent, cell division within the VE is Nodal independent. To confirm that proliferation in the epiblast is indeed reduced after inhibition of Nodal signalling, PH3 staining was carried out on SB-431542-treated embryos (Fig. 5C,D). Blocking Nodal signalling caused a significant reduction in the number of mitotic cells in the epiblast, with control embryos having a mean mitotic index of 7.85±0.64% and SB-431542-treated embryos a mean mitotic index of 4.21±0.4% ($P < 0.0001$). The possibility that epiblast cells exit from the cell cycle after SB-431542 treatment was supported by the observation that expression of *c-Myc* was also lost from the epiblast after inhibition of Nodal signalling (see Fig. S4A' in the supplementary material).

Nodal signalling is required to induce the AVE (Brennan et al., 2001), so one explanation for the lack of AVE migration after inhibition of Nodal signalling is a failure to maintain the identity of this tissue. The expression of the AVE markers *Dkk1*, *Lim1*

(*Lhx1* – Mouse Genome Informatics) and *Cer11* and the proximal VE markers *Hnf4* and *Gata4* were analysed in 5.5-dpc embryos after treatment with SB-431542. There was a loss of expression of all the AVE markers (see Fig. S4B-D' in the supplementary material), an expansion in *Hnf4* expression (see Fig. S4F' in the supplementary material) and a strong downregulation in the expression of *Gata4*, as compared with control embryos (see Fig. S4E' in the supplementary material). The loss of expression of AVE markers and the upregulation of *Hnf4* in the distal VE indicate that Nodal signalling is required not only for AVE induction but also for the maintenance of AVE identity in these cells. Therefore, Nodal signalling is required for the maintenance of proliferation in the epiblast and for expression of AVE markers in the VE.

Fig. 5. Nodal signalling is required for epiblast proliferation and AVE migration. (A,A') BrdU staining of control cultured *Hex*-GFP 5.5-dpc mouse embryos (A) and *Hex*-GFP embryos cultured overnight in the presence of the Nodal receptor inhibitor SB-431542 (10 μ M) (A'). (B) BrdU-incorporation index of the epiblast (Epi), AVE and posterior VE (PVE) of control ($n=11$) and SB-431542-treated ($n=14$) embryos. (C,C') PH3 staining of control cultured *Hex*-GFP 5.5-dpc embryos (C) and *Hex*-GFP embryos cultured overnight in 10 μ M SB-431542 (C'). (D) Mean mitotic index in the epiblast of control ($n=16$) and SB-431542-treated ($n=17$) embryos. (E,E') PH3 staining of 5.5-dpc control (E) and *Cripto* mutant (E') embryos. (F) Mean mitotic index for the epiblast and VE of control ($n=21$) and *Cripto*-null ($n=8$) embryos. All results are mean \pm s.e.m. * $P < 0.05$, ** $P < 0.01$ by Student's *t*-test.

Nodal-driven proliferation in the epiblast is required for AVE migration

The misspecification of AVE markers is likely to be one cause for the AVE migration defects observed after inhibition of Nodal signalling, but this does not exclude the possibility that Nodal-driven proliferation in the epiblast is also required for AVE migration. To test this possibility, we studied embryos mutant for the Nodal co-receptor *Cripto* (*Tdgfl* – Mouse Genome Informatics), which specify a DVE, but the DVE does not migrate to the prospective anterior (Fig. 5E,F) (Ding et al., 1998). The mitotic index of the VE of *Cripto*-null embryos (2.92±0.92%) was similar to that of the controls (2.13±0.5%); however, in the epiblast, the mitotic index of *Cripto* mutant embryos (3.76±0.38%) was significantly lower than that of controls (6.75±0.82%; $P < 0.05$). Given that *Cripto* is required in the epiblast for the migration of the AVE (Kimura et al., 2001), this suggests that this defect in epiblast proliferation could contribute to the migration defects observed in *Cripto* mutant embryos.

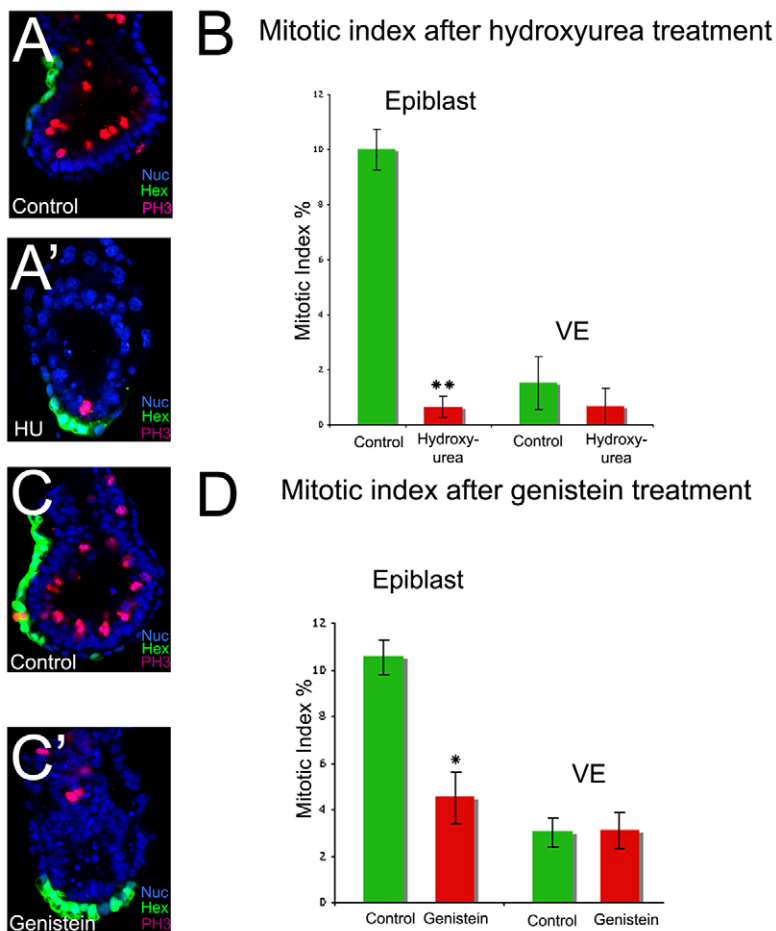


Fig. 6. Proliferation in the epiblast is required for the migration of the AVE. (A,A') PH3 staining of control (A) and hydroxyurea-treated (A') *Hex*-GFP mouse embryos. (B) Mean mitotic index in the epiblast and VE of control ($n=6$) and hydroxyurea-treated ($n=7$) embryos. (C,C') PH3 staining of control (C) and genistein-treated (C') embryos ($n=8$ for both). (D) Mean mitotic index in the epiblast and VE of control ($n=8$) and non-migrated genistein-treated ($n=8$) embryos. All results are mean \pm s.e.m.; * $P<0.05$, ** $P<0.01$, Student's *t*-test.

To confirm this result, we cultured 5.5-dpc embryos for 2 hours with the Nodal receptor inhibitor SB-431542 when AVE movements are just being initiated. During the first phase of inhibition of Nodal signalling, we observed no change in the expression of AVE markers, nor in the expression of general VE markers (see Fig. S5A-D' in the supplementary material). By contrast, we observed a significant decrease in the proliferation rate of the epiblast but not of the VE (see Fig. S5E-F in the supplementary material). These data suggest that during the first 2 hours of Nodal signalling inhibition, the primary process that is affected is proliferation rather than AVE specification. As it is during this period that the AVE movements are initiated, these results show that Nodal-driven proliferation in the epiblast affects AVE migration.

To test whether proliferation in the epiblast is required for AVE migration, cell cycle inhibitors were used. *Hex*-GFP embryos at 5.5 dpc were cultured overnight in the presence of the mitotic inhibitor nocodazole (200 nM) (MacAuley et al., 1993). This resulted in a block in AVE migration ($n=16/18$; data not shown) and in at least a 3-fold accumulation of cells in M phase (Fig. 2E), suggesting that proliferation is indeed required for AVE migration. To confirm these results, two other cell cycle inhibitors were tested: hydroxyurea, which blocks cells in S phase (Engstrom et al., 1979), and genistein, a tyrosine kinase inhibitor that blocks the G_2 -M transition (Matsukawa et al., 1993). Embryos cultured in 2.5 μ M hydroxyurea showed a lack of AVE migration ($n=15/17$; Fig. 6A') and displayed a 93.6% reduction in the number of mitotic cells in the epiblast (controls, $10.00 \pm 0.73\%$; hydroxyurea treated,

$0.64 \pm 0.39\%$; $P<0.0001$; Fig. 6B). There was no significant difference in the number of mitotic cells in the VE of these embryos (controls, $1.51 \pm 0.96\%$; hydroxyurea treated, $0.67 \pm 0.67\%$; Fig. 6B). Similarly, embryos cultured in 150 μ M genistein also presented a failure of AVE migration ($n=7/11$; Fig. 6C,C') and a significant decrease in mitotic cells in the epiblast (controls, $10.54 \pm 0.75\%$; genistein treated, $4.51 \pm 1.1\%$; Fig. 6D; $P<0.0005$) but not within the VE (controls, $3.11 \pm 0.79\%$; genistein treated, $3.02 \pm 0.62\%$; Fig. 6D). Given that neither AVE nor VE markers are affected by any of these inhibitors (see Fig. S6 in the supplementary material), these results indicate that proliferation is required for AVE migration and strongly suggest that it is proliferation in the epiblast that is required for these cell movements.

AVE cells have been shown to move away from a repulsive Wnt signal and towards a Dkk1 attractant signal (Kimura-Yoshida et al., 2005). A possible explanation as to how epiblast proliferation facilitates AVE migration is by moving the prospective AVE cells (DVE) away from the inhibitory Wnt signals. To test this hypothesis, embryos were cultured in the presence of nocodazole to inhibit proliferation and of Dkk1 as an AVE attractant. We found that only 3% ($n=1/31$) of nocodazole-treated embryos showed a migrated AVE and 35% ($n=11/31$) showed partial AVE movements, whereas in those embryos cultured in the presence of nocodazole and Dkk1 33% ($n=11/33$) showed a migrated AVE and 55% ($n=18/33$) displayed partial migration (Fig. 7). Interestingly, in the majority of these latter embryos migration seemed to have occurred unilaterally, suggesting that the cues for the direction of

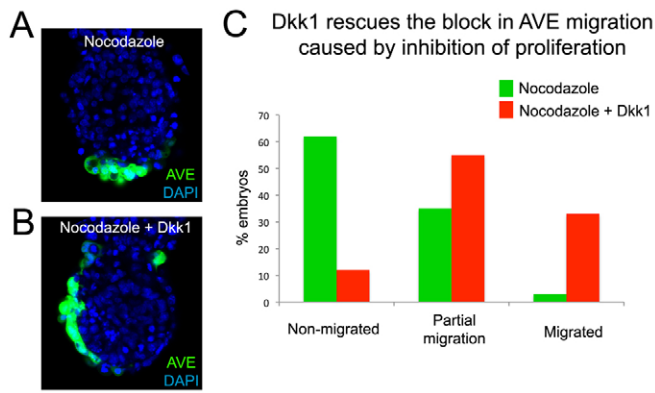


Fig. 7. Dkk1 rescues the block in AVE migration caused by inhibition of proliferation. (A,B) 5.5-dpc mouse embryos cultured overnight in the presence of nocodazole (A; $n=31$) or nocodazole and Dkk1 (B; $n=33$). (C) The percentage of embryos with a migrated, partially migrated or non-migrated AVE for those treated with nocodazole versus nocodazole plus Dkk1.

AVE movements had already been provided at the starting point of our cultures. These results indicate that the AVE migration defects caused by inhibiting proliferation can be rescued by Dkk1, and support the argument that the proliferation in the epiblast has a facilitative role for the AVE movements by moving the DVE away from signals that are inhibitory to its migration.

DISCUSSION

Little is known about how the growth of the embryo and patterning are integrated during early mammalian development. We have shown that epiblast proliferation is required to facilitate the initiation of AVE migration. This provides a mechanism to ensure that during post-implantation development, the rate of embryonic growth is tightly associated with the development of axial patterning.

Differential proliferation within the VE and AVE migration

Active migration (Srinivas et al., 2004) and passive displacement due to differential proliferation within the VE (Yamamoto et al., 2004) have both been proposed as forces that drive AVE movements. We have carried out a detailed analysis of the distribution of proliferation within the VE at the different stages of AVE migration and found that there is no evidence for differential cell division at any stage of this process between the anterior and posterior VE. A number of other studies support our findings. First, the DVE cells reach the embryonic/extra-embryonic boundary in as little as 4-5 hours, leaving cells behind at the distal tip of the embryo (Srinivas et al., 2004). Second, the average cell cycle length in the VE at the time of the DVE movements is estimated to be over 16 hours (Snow, 1977). Third, detailed analyses of clonal populations in the VE prior to gastrulation fail to outline major differences in proliferation rates between the four subregions of the distal VE (Perea-Gomez et al., 2001). In contrast to these findings, a previous study reported an absence of BrdU incorporation in the AVE, suggesting differential proliferation between the anterior and posterior VE (Yamamoto et al., 2004). It is possible that the difference between this and our study could be explained by a lower sensitivity of the protocol used to detect BrdU or variations in the genetic strains used.

The hypothesis that cell migration is the main motive force driving AVE movements is supported by the lack of any difference in proliferation rates in the VE, as well as by a number of other recent observations. Time-lapse imaging showing the dynamics of AVE movements (Srinivas et al., 2004), studies identifying attractants for these movements (Kimura-Yoshida et al., 2005) and the finding that embryos carrying mutations in genes that are essential for cell migration exhibit defective AVE movements (Migeotte et al., 2010; Rakeman and Anderson, 2006) all support this hypothesis.

Analysis of the distribution of proliferating cells at 5.5 dpc revealed that the right side of the embryo is proliferating at a significantly higher rate than the left side at this stage. Between 5.5 and 6.5 dpc there is a change in the orientation of the axis of bilateral symmetry of the embryo, an event that is thought to be required for the initiation of gastrulation (Mesnard et al., 2004; Perea-Gomez et al., 2004). Given that this change in axis of symmetry does not appear to involve cell movements (Perea-Gomez et al., 2004), it is tempting to speculate that it might be driven by differential proliferation between the left and right sides of the embryo.

Coordination between epiblast proliferation and establishment of the A-P axis

During development, the growth of the embryo must be coordinated with its morphogenesis to ensure that patterning occurs in a correct and timely fashion. Here, we show that epiblast growth is directly linked to the initiation of AVE movements, an essential step for the correct establishment of the A-P axis.

Several lines of evidence suggest that proliferation in the epiblast is required for the initiation of AVE movements. First, as AVE movements are being initiated the growth imbalance between the epiblast and the VE grows from 2.2-fold to 11-fold and drops again once the A-P axis has been established. Second, after inhibition of Nodal signalling during the first phase of AVE migration, and in *Cripto* mutants in which the AVE forms but does not migrate, we see a decrease in the cell division rate in the epiblast but not in the VE. Third, genistein and hydroxyurea caused AVE migration defects and efficiently inhibited proliferation in the epiblast but failed to do so in the VE. These observations clearly indicate that proliferation in the epiblast is required for AVE migration. The specific loss of cell division that occurs in the epiblast after inhibition of Nodal signalling by SB-435142, as well as in *Cripto* mutants, clearly points to Nodal signalling as a major player in the control of embryonic growth. A critical target of Nodal signalling during this process is likely to be *c-Myc*, given the downregulation we observe in the epiblast expression of this gene after inhibition of Nodal signalling.

How does proliferation in the epiblast affect AVE movements? AVE cells have been shown to move away from a repulsive Wnt signal and towards an attractive Dkk1 signal (Kimura-Yoshida et al., 2005). We show that Dkk1 can rescue the AVE migration defects caused by inhibition of proliferation. This suggests that proliferation plays a facilitative role for AVE migration by moving the prospective AVE cells (DVE) away from signals that inhibit its migration.

The requirement for epiblast proliferation in the initiation of AVE migration is not the only control mechanism that ensures coordination of embryonic growth and A-P patterning. Indeed, the induction of the AVE requires a certain embryo size to ensure that the distal tip of the embryo is sufficiently distant from the inhibitory signals of the extra-embryonic ectoderm (Mesnard et al., 2006) and

a critical cell number within the epiblast is required for the initiation of gastrulation (Power and Tam, 1993; Snow, 1977; Tam and Behringer, 1997). Therefore, it is becoming clear that during post-implantation development, a complex set of checkpoints exists to ensure that morphogenesis and growth go hand in hand.

In conclusion, we report that prior to, and during, AVE movements, there is no evidence for differential proliferation within the VE and it is therefore likely that cell migration is the driving force for AVE movements. We have identified a novel checkpoint control that links growth of the embryo with establishment of the A-P axis. This checkpoint ensures a coupling of the migration of the AVE to the Nodal-driven proliferation in the epiblast and therefore ensures that the patterning in both the epiblast and VE are coordinated.

Acknowledgements

We thank Michael Shen for the *Cripto*^{+/−} mice; Yi-Ping Li, Daniel Constam, William Shawlot, José Belo and Christof Niehrs for kindly providing plasmids; and Francis Vella for helpful discussion. T.A.R. holds a Lister Institute of Preventative Medicine Fellowship and this work was also supported by the Medical Research Council. Deposited in PMC for release after 6 months.

Competing interests statement

The authors declare no competing financial interests.

Supplementary material

Supplementary material for this article is available at <http://dev.biologists.org/lookup/suppl/doi:10.1242/dev.063537/-/DC1>

References

- Ben-Haim, N., Lu, C., Guzman-Ayala, M., Pescatore, L., Mesnard, D., Bischofberger, M., Naef, F., Robertson, E. J. and Constam, D. B. (2006). The nodal precursor acting via activin receptors induces mesoderm by maintaining a source of its convertases and BMP4. *Dev. Cell* **11**, 313–323.
- Brennan, J., Lu, C. C., Norris, D. P., Rodriguez, T. A., Beddington, R. S. and Robertson, E. J. (2001). Nodal signalling in the epiblast patterns the early mouse embryo. *Nature* **411**, 965–969.
- Camus, A., Perea-Gomez, A., Moreau, A. and Collignon, J. (2006). Absence of nodal signaling promotes precocious neural differentiation in the mouse embryo. *Dev. Biol.* **295**, 743–755.
- Chenn, A. and Walsh, C. A. (2002). Regulation of cerebral cortical size by control of cell cycle exit in neural precursors. *Science* **297**, 365–369.
- Connolly, K. M. and Bogdanffy, M. S. (1993). Evaluation of proliferating cell nuclear antigen (PCNA) as an endogenous marker of cell proliferation in rat liver: a dual-stain comparison with 5-bromo-2'-deoxyuridine. *J. Histochem. Cytochem.* **41**, 1–6.
- Di-Gregorio, A., Sancho, M., Stuckey, D. W., Crompton, L. A., Godwin, J., Mishina, Y. and Rodriguez, T. A. (2007). BMP signalling inhibits premature neural differentiation in the mouse embryo. *Development* **134**, 3359–3369.
- Ding, J., Yang, L., Yan, Y. T., Chen, A., Desai, N., Wynshaw-Boris, A. and Shen, M. M. (1998). *Cripto* is required for correct orientation of the anterior-posterior axis in the mouse embryo. *Nature* **395**, 702–707.
- DiPaola, R. S. (2002). To arrest or not to G(2)-M Cell-cycle arrest: commentary re: A. K. Tyagi et al., Silibinin strongly synergizes human prostate carcinoma DU145 cells to doxorubicin-induced growth inhibition, G(2)-M arrest, and apoptosis. *Clin. Cancer Res.* **8**, 3512–3519, 2002. *Clin. Cancer Res.* **8**, 3311–3314.
- Engstrom, Y., Eriksson, S., Thelander, L. and Akerman, M. (1979). Ribonucleotide reductase from calf thymus. Purification and properties. *Biochemistry* **18**, 2941–2948.
- Inman, G. J., Nicolas, F. J., Callahan, J. F., Harling, J. D., Gaster, L. M., Reith, A. D., Laping, N. J. and Hill, C. S. (2002). SB-431542 is a potent and specific inhibitor of transforming growth factor-beta superfamily type I activin receptor-like kinase (ALK) receptors ALK4, ALK5, and ALK7. *Mol. Pharmacol.* **62**, 65–74.
- Kimura, C., Shen, M. M., Takeda, N., Aizawa, S. and Matsuo, I. (2001). Complementary functions of *Otx2* and *Cripto* in initial patterning of mouse epiblast. *Dev. Biol.* **235**, 12–32.
- Kimura-Yoshida, C., Nakano, H., Okamura, D., Nakao, K., Yonemura, S., Belo, J. A., Aizawa, S., Matsui, Y. and Matsuo, I. (2005). Canonical Wnt signaling and its antagonist regulate anterior-posterior axis polarization by guiding cell migration in mouse visceral endoderm. *Dev. Cell* **9**, 639–650.
- MacAuley, A., Werb, Z. and Mirkes, P. E. (1993). Characterization of the unusually rapid cell cycles during rat gastrulation. *Development* **117**, 873–883.
- Matsukawa, Y., Marui, N., Sakai, T., Satomi, Y., Yoshida, M., Matsumoto, K., Nishino, H. and Aoike, A. (1993). Genistein arrests cell cycle progression at G2-M. *Cancer Res.* **53**, 1328–1331.
- Mesnard, D., Filipe, M., Belo, J. A. and Zernicka-Goetz, M. (2004). The anterior-posterior axis emerges respecting the morphology of the mouse embryo that changes and aligns with the uterus before gastrulation. *Curr. Biol.* **14**, 184–196.
- Mesnard, D., Guzman-Ayala, M. and Constam, D. B. (2006). Nodal specifies embryonic visceral endoderm and sustains pluripotent cells in the epiblast before overt axial patterning. *Development* **133**, 2497–2505.
- Migeotte, I., Omelchenko, T., Hall, A. and Anderson, K. V. (2010). Rac1-dependent collective cell migration is required for specification of the anterior-posterior body axis of the mouse. *PLoS Biol.* **8**, e1000442.
- Mishina, Y., Suzuki, A., Ueno, N. and Behringer, R. R. (1995). *Bmpr* encodes a type I bone morphogenetic protein receptor that is essential for gastrulation during mouse embryogenesis. *Genes Dev.* **9**, 3027–3037.
- Nagy, A., Gertsenstein, M., Vintersten, K. and Behringer, R. (2003). *Manipulating the Mouse Embryo*. Cold Spring Harbor, New York: Cold Spring Harbor Laboratory Press.
- Norris, D. P., Brennan, J., Bikoff, E. K. and Robertson, E. J. (2002). The *Foxh1*-dependent autoregulatory enhancer controls the level of Nodal signals in the mouse embryo. *Development* **129**, 3455–3468.
- Perea-Gomez, A., Rhinn, M. and Ang, S. L. (2001). Role of the anterior visceral endoderm in restricting posterior signals in the mouse embryo. *Int. J. Dev. Biol.* **45**, 311–320.
- Perea-Gomez, A., Camus, A., Moreau, A., Grieve, K., Moneron, G., Dubois, A., Cibert, C. and Collignon, J. (2004). Initiation of gastrulation in the mouse embryo is preceded by an apparent shift in the orientation of the anterior-posterior axis. *Curr. Biol.* **14**, 197–207.
- Power, M. A. and Tam, P. P. (1993). Onset of gastrulation, morphogenesis and somitogenesis in mouse embryos displaying compensatory growth. *Anat. Embryol. (Berl.)* **187**, 493–504.
- Rakeman, A. S. and Anderson, K. V. (2006). Axis specification and morphogenesis in the mouse embryo require *Nap1*, a regulator of WAVE-mediated actin branching. *Development* **133**, 3075–3083.
- Rodriguez, T. A., Casey, E. S., Harland, R. M., Smith, J. C. and Beddington, R. S. (2001). Distinct enhancer elements control *Hex* expression during gastrulation and early organogenesis. *Dev. Biol.* **234**, 304–316.
- Rodriguez, T. A., Srinivas, S., Clements, M. P., Smith, J. C. and Beddington, R. S. (2005). Induction and migration of the anterior visceral endoderm is regulated by the extra-embryonic ectoderm. *Development* **132**, 2513–2520.
- Sakaue-Sawano, A., Kurokawa, H., Morimura, T., Hanyu, A., Hama, H., Osawa, H., Kashiwagi, S., Fukami, K., Miyata, T., Miyoshi, H. et al. (2008). Visualizing spatiotemporal dynamics of multicellular cell-cycle progression. *Cell* **132**, 487–498.
- Snow, M. H. L. (1977). Gastrulation in the mouse: growth and regionalization of the epiblast. *J. Embryol. Exp. Morphol.* **42**, 293–303.
- Srinivas, S. (2006). The anterior visceral endoderm-turning heads. *Genesis* **44**, 565–572.
- Srinivas, S., Rodriguez, T., Clements, M., Smith, J. C. and Beddington, R. S. (2004). Active cell migration drives the unilateral movements of the anterior visceral endoderm. *Development* **131**, 1157–1164.
- Takahashi, T. and Caviness, V. S., Jr (1993). PCNA-binding to DNA at the G1/S transition in proliferating cells of the developing cerebral wall. *J. Neurocytol.* **22**, 1096–1102.
- Takaoka, K., Yamamoto, M. and Hamada, H. (2007). Origin of body axes in the mouse embryo. *Curr. Opin. Genet. Dev.* **17**, 344–350.
- Tam, P. P. and Behringer, R. R. (1997). Mouse gastrulation: the formation of a mammalian body plan. *Mech. Dev.* **68**, 3–25.
- Thomas, P. and Beddington, R. (1996). Anterior primitive endoderm may be responsible for patterning the anterior neural plate in the mouse embryo. *Curr. Biol.* **6**, 1487–1496.
- Vasquez, R. J., Howell, B., Yvon, A. M., Wadsworth, P. and Cassimeris, L. (1997). Nanomolar concentrations of nocodazole alter microtubule dynamic instability in vivo and in vitro. *Mol. Biol. Cell* **8**, 973–985.
- Yamamoto, M., Saijoh, Y., Perea-Gomez, A., Shawlot, W., Behringer, R. R., Ang, S. L., Hamada, H. and Meno, C. (2004). Nodal antagonists regulate formation of the anteroposterior axis of the mouse embryo. *Nature* **428**, 387–392.
- Yamamoto, M., Beppu, H., Takaoka, K., Meno, C., Li, E., Miyazono, K. and Hamada, H. (2009). Antagonism between *Smad1* and *Smad2* signaling determines the site of distal visceral endoderm formation in the mouse embryo. *J. Cell Biol.* **184**, 323–334.

Table S1. Total number of PH3-positive (mitotic) cells over the total number of cells analysed in the VE

Group	<i>n</i>	Region	PH3 ⁺ /total
Pre-distal	5	VE	18/532
Distal	6	DVE	4/166
		emVE	4/265
		exeVE	5/283
Tilted	5	AVE	3/263
		Posterior VE	5/289
		Left VE	1/198
		Right VE	2/238
Migrated	8	AVE	7/376
		Posterior VE	5/324
		Left VE	4/269
		Right VE	5/290

The mitotic indexes were calculated by dividing the number of mitotic cells by the total number of cells analysed for each region for each embryo. The average of these individual embryo mitotic indexes is presented in the text and figures as the overall mitotic index.